ChemComm

Photochemical hydrogen production based on HCOOH/CO2 cycle promoted by pentanuclear cobalt complex

Journal:	*ChemComm*
Manuscript ID	CC-COM-11-2021-006445.R1
Article Type:	Communication

COMMUNICATION

Photochemical hydrogen production based on HCOOH/CO_2 cycle promoted by pentanuclear cobalt complex

Received 00th January 20xx,
Accepted 00th January 20xx

DOI: 10.1039/x0xx00000x

Takuya Akai,[a] Mio Kondo,[abc] Yutaka Saga[ac] and Shigeyuki Masaoka*[ac]

The first catalytic cycle for hydrogen production based on the photochemical two-electron reduction of carbon dioxide (CO_2) and the dehydrogenation of formic acid at ambient temperature was demonstrated using a pentanuclear cobalt complex (Co5). A series of mechanistic studies were performed to elucidate the mechanism responsible for the promotion of the photocatalytic cycle by Co5.

With the increasing demand for energy and the rapid depletion of fossil fuels, the development of renewable and environmentally friendly energy sources has become essential. In this respect, hydrogen gas is a promising energy carrier and a clean alternative to conventional fossil fuels. However, its gaseous nature and low volumetric energy density make it difficult to store and transport. Given this background, significant research efforts have focused on the liquid organic hydrogen carrier formic acid, which is a low-toxicity liquid under ambient conditions.[1] Its ease of storage and transportation and high volumetric energy density make it a viable hydrogen carrier. Therefore, efficient catalysts for the production of formic acid and its conversion into hydrogen are required for utilisation of formic acid as a hydrogen carrier.

Catalysts that promote release of hydrogen via the dehydrogenation of formic acid have been studied extensively.[1, 2] In this catalytic reaction, formic acid is converted into molecular hydrogen and carbon dioxide (HCOOH → H_2 + CO_2). By recycling the formed CO_2 back into formic acid, a carbon-neutral cycle can be realised (Fig. 1). To date, several catalysts that allow for reversible dehydrogenation/hydrogenation (CO_2 + H_2 → HCOOH) between formic acid and CO_2 (Fig. 1(a)) have been reported.[1,3] Nevertheless, this cycling process involves the utilisation of gaseous hydrogen and generally harsh reaction

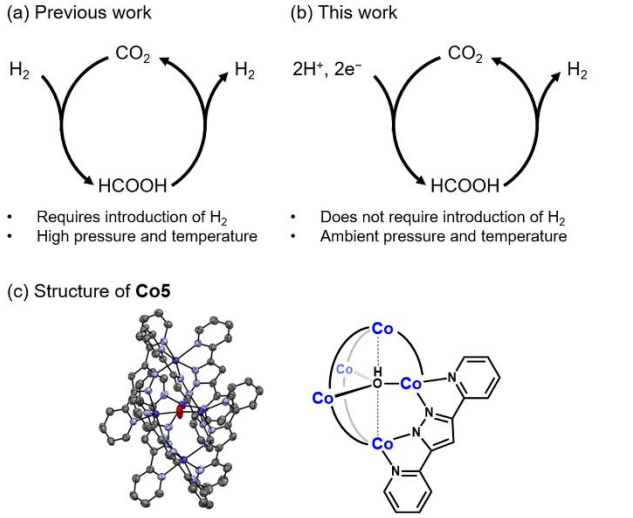

Fig. 1 (a), (b) Two distinct H_2 storage/release cycles that use formic acid as hydrogen carrier. (a) CO_2 hydrogenation and HCOOH dehydrogenation couple. (b) CO_2 reduction and HCOOH dehydrogenation couple. (c) Structure of $[Co_5OH(bpp)_6]^{3+}$ (**Co5**, Hbpp = 3,5-bis(2-pyridyl)pyrazole).

conditions (high pressure and/or heating)[3,4] for storing the hydrogen in the form of formic acid (hydrogenation process). Another method for obtaining formic acid from CO_2 is the two-electron reduction of CO_2 in the presence of protons (CO_2 + $2H^+$ + $2e^-$ → HCOOH). There have been a number of reports on catalysts that promote the photo- and electrochemical reduction of CO_2 into formic acid under ambient conditions.[5] However, there are no reports on catalysts that can promote both the reduction of CO_2 and the dehydrogenation of formic acid (Fig. 1(b)).

Herein, we report the first example of a catalyst that shows catalytic activity for both the reduction of CO_2 and the dehydrogenation of formic acid. A pentanuclear cobalt complex, $[Co^{II}_5OH(bpp)_6]^{3+}$, (**Co5**, Hbpp = 3,5-bis(2-pyridyl)pyrazole), see Fig. 1(c)), which was previously reported by us and can catalyse the photochemical reduction of CO_2 to produce formic acid[6], was found to also catalyse the photoinduced dehydrogenation of formic acid at ambient temperature. Under the optimised

[a] *Division of Applied Chemistry, Graduate School of Engineering, Osaka University, 2-1 Yamadaoka, Suita, Osaka 565-0871, Japan. E-mail: masaoka@chem.eng.osaka-u.ac.jp*
[b] *JST, PRESTO, 4-1-8 Honcho, Kawaguchi, Saitama 332-0012, Japan.*
[c] *Innovative Catalysis Science Division, Institute for Open and Transdisciplinary Research Initiatives (ICS-OTRI), Osaka University, Suita, Osaka 565-0871, Japan.*
†Electronic Supplementary Information (ESI) available: [Experimental details and supplementary data]. See DOI: 10.1039/x0xx00000x

conditions, the turnover frequency (TOF) of **Co5** for the dehydrogenation reaction of formic acid was higher (229 h^{-1}) than those reported for other molecular catalysts that operate under photoirradiation at ambient temperature. In addition, mechanistic studies were performed to elucidate the underlying mechanism of the catalytic cycle, and the critical role of the Co^{I} species of **Co5** both in the formic acid dehydrogenation reaction and the CO_2 reduction process was clarified. The results of this study should aid the development of new carbon-neutral energy cycles that use formic acid as a hydrogen carrier.

Our study begins with a serendipitous finding upon examining the photocatalytic activity of **Co5** for CO_2 reduction. During this experiment, the photoirradiation of a solution containing **Co5**, a photosensitiser, a proton source and a sacrificial electron donor in a CO_2 atmosphere resulted in the formation of formic acid, carbon monoxide, and hydrogen (Fig. S1). Surprisingly, the evolution of hydrogen was completely suppressed in an Ar atmosphere, indicating that CO_2 is required for the generation of hydrogen. Given this observation, we assumed that the evolution of hydrogen originates from dehydrogenation of formic acid and not proton reduction.

Encouraged by the aforementioned result, we investigated the suitability of **Co5** as a catalyst for the dehydrogenation of formic acid under photoirradiation. The initial reaction was performed in 2 mL of an *N,N*-dimethylacetamide (DMA) solution containing **Co5** (30 μM) as the catalyst, $Ir(ppy)_3$ (Hppy = 2-phenylpyridine, 150 μM) as the photosensitiser, 1,3-dimethyl-2-phenyl-2,3-dihydro-1*H*-benzo[*d*]imidazole (BIH, 0.1 M) as the sacrificial electron donor, and formic acid (500 *eq. versus* **Co5**) as the substrate in an Ar atmosphere under irradiation with visible light (blue LED, wavelength λ = 420 nm) at 20 °C. As shown in Fig. 2, the evolution of hydrogen gas was observed after 3 h of photoirradiation. This result implies that **Co5** can catalyse the photoinduced dehydrogenation of formic acid at ambient temperature.

A series of control experiments was performed to further investigate the catalytic reaction. First, a reaction was performed using trifluoroacetic acid (TFA) instead of formic acid as a substrate. Only a small amount of hydrogen was detected (Table S1, No. 2), confirming that proton reduction cannot proceed under these conditions. In addition, reactions in the absence of **Co5**, $Ir(ppy)_3$, BIH, or light irradiation yielded hydrogen in trace amounts (Fig. 2 and Table S1). Therefore, all the above-mentioned components are required to promote the dehydrogenation of formic acid. These facts confirmed that **Co5** is suitable for use as a catalyst for the photochemical dehydrogenation of formic acid at ambient temperature. Note that this is one of the few instances of the dehydrogenation of formic acid under photoirradiation.[2d,h,i,k,l,o,]

Subsequently, the effects of the individual components on the catalytic performance of the system were examined. First, we performed the dehydrogenation reactions using different photosensitisers [Figs. 3(a, b)], namely, $Ir(ppy)_3$, $[Ir(dtbbpy)(ppy)_2](PF_6)$ (**Ir-2**, dtbbpy = 4,4′-di-*t*-butyl-2,2′-bipyridine), and $[Ir(dF(CF_3)ppy)_2(dtbbpy)](PF_6)$ (**Ir-3**, $dF(CF_3)ppy$ = 2-(2,4-difluorophenyl)-5-(trifluoromethyl) pyridine). The reactions that used $Ir(ppy)_3$ and **Ir-2** as the photosensitiser

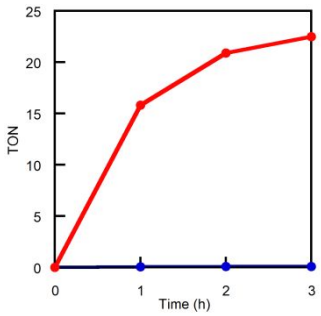

Fig. 2 Photochemical production of H_2 in presence of 30 μM **Co5** (red line) and in absence of **Co5** (blue line) in Ar-saturated DMA solution containing 150 μM $Ir(ppy)_3$, 100 mM BIH, and 13 mM formic acid at 20 °C.

resulted in the formation of hydrogen, whereas no hydrogen was detected when **Ir-3** was used (Fig. 3(b)). Of the three photosensitisers tested, $Ir(ppy)_3$ exhibited the highest efficiency for the dehydrogenation of formic acid. Thus, we employed the complex as the photosensitiser for the subsequent investigations. Next, the effect of the concentration of the photosensitiser, that is, $Ir(ppy)_3$, was investigated. The evolution of hydrogen accelerated with an increase in the concentration of $Ir(ppy)_3$ (Fig. 3(c)), suggesting that the dehydrogenation of formic acid in the proposed system occurred readily at higher $Ir(ppy)_3$ concentrations. Finally, the effect of the concentration of the sacrificial electron donor (BIH) was investigated. As shown in Fig. 3(d), as the concentration of BIH was increased, the amount of hydrogen generated decreased dramatically, indicating that the presence of BIH in a higher concentration hindered the dehydrogenation reaction.

Based on these results, we were able to gain additional insights into the reaction mechanism. The choice of the photosensitiser greatly affects the efficiency of the system (see above). This result can be explained based on the reduction potentials. The first reduction potentials, $E_{1/2}(Ir^{III}/Ir^{II})$, of the investigated photosensitisers are −2.64 ($Ir(ppy)_3$), −1.87 (**Ir-2**) and −1.74 V (**Ir-3**) (*versus* Fc/Fc^+ (ferrocene/ferrocenium), see Table S2). As we had reported previously[6], **Co5** exhibits a one-electron reduction wave at $E_{1/2}(Co^{II}{}_5/Co^{II}{}_4Co^{I}) = -1.72$ V (*versus* Fc/Fc^+), which is attributable to the reduction of the cobalt centre at the triangular core (for details of the assignment of redox peaks, see the ESI (P. S7)). A comparison of the redox potentials of the investigated photosensitisers and **Co5** revealed that $Ir(ppy)_3$ and **Ir-2** were able to reduce **Co5** during the photocatalytic reaction while **Ir-3** was not. As mentioned earlier, the reactions involving $Ir(ppy)_3$ and **Ir-2** resulted in hydrogen production, whereas that that used **Ir-3** as the photosensitiser did not. These results indicate that the one-electron-reduced species of **Co5** was involved in the reaction.

To confirm this hypothesis, cyclic voltammetry (CV) was performed in the presence of **Co5** and formic acid. The current at the first reduction peak of **Co5** was slightly higher compared with that in the absence of formic acid (Fig. S4). It should also be noted that this current enhancement was not observed when TFA was added to the solution (Fig. S5). Thus, the cyclic voltammograms indicated that specific interactions occur between the one-electron reduced species of **Co5** and formic

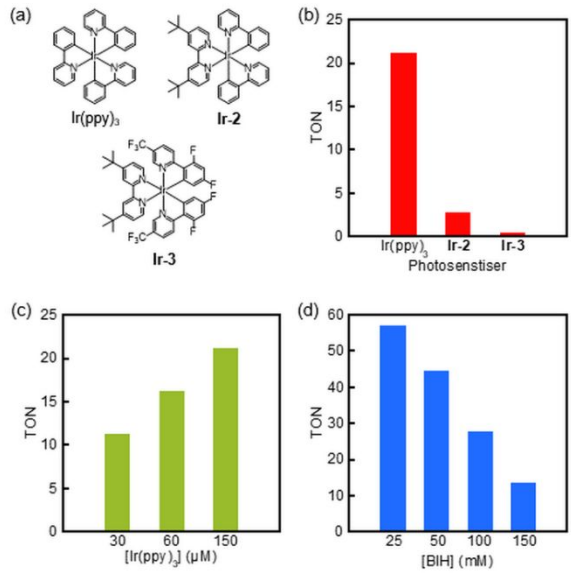

Fig. 3 (a) Structures and (b) photochemical formic acid dehydrogenation activities of different photosensitisers: $Ir(ppy)_3$, **Ir-2**, and **Ir-3**. Effects of concentrations of (c) $Ir(ppy)_3$ and (d) BIH. Reactions were performed in DMA solution containing 30 μM **Co5**, 13 mM formic acid and (b) 150 μM photosensitiser and 100 mM BIH, (c) 30–150 μM $Ir(ppy)_3$ and 100 mM BIH, and (d) 150 μM $Ir(ppy)_3$ and 25–150 mM BIH.

acid. Therefore, the Co^I present at the triangular core plays a critical role in the reaction. This conclusion is consistent with the fact that all the previous examples of formic acid dehydrogenation reactions mediated by cobalt complexes were triggered by the Co^I species.[2d,n]

Next, the effect of the concentration of $Ir(ppy)_3$ is discussed. As mentioned above, the formation of Co^I at the triangular core via the photoinduced one-electron reduction of **Co5** is essential for the reaction. Therefore, it was expected that an increase in the concentration of $Ir(ppy)_3$ would increase the rate of photoinduced electron transfer. In fact, the amount of hydrogen evolved increased when the amount of $Ir(ppy)_3$ added to the reaction medium was increased (see above). In other words, the concentration of $Ir(ppy)_3$ has a determining effect on the frequency of the photoinduced electron transfer events. Note that the concentrations of $Ir(ppy)_3$ employed in our photocatalytic investigations are low enough that all the incident photons were not absorbed; the fraction of light absorbed during the photocatalytic experiment is in the range from 53 % to 98%.

The effect of the concentration of BIH on the catalysis process can be understood based on the photoinduced electron transfer pathway for the formation of the key intermediate, namely, the one-electron reduced species of **Co5** with Co^I at the triangular core. There are two possible pathways for accessing this species. The first pathway is the reductive quenching of $Ir(ppy)_3$ by BIH and the subsequent reduction of **Co5** by formed one-electron reduced species of $Ir(ppy)_3$. The second pathway is the oxidative quenching of $Ir(ppy)_3$ by **Co5**, resulting in the one-electron reduced state of **Co5**. To elucidate the photoinduced electron transfer pathway during catalysis, we examined the rates of quenching of the excited-state photosensitiser $Ir(ppy)_3$ by **Co5** (oxidative quenching) and BIH (reductive quenching) using Stern–Volmer plots. Upon increasing the concentration of **Co5**/BIH in a solution of $Ir(ppy)_3$, emission quenching was observed (Fig. S6). The corresponding quenching rate constants for the oxidative and reductive quenching pathways were determined to be k_q = 6.6 x 10^9 and 5.5 x 10^6 M^{-1} s^{-1}, respectively. Considering that the concentration of BIH is approximately 10^3 times higher than that of **Co5** in the proposed photocatalytic reaction, the rates of the two quenching pathways are comparable. At a BIH concentration of 50 mM, the calculated oxidative and reductive quenching rates are almost identical. In addition, the experimental results showed clearly that the catalysis reaction is deaccelerated when BIH is added in a higher concentration (Fig. 3(d)). Oxidative quenching was dominant at lower BIH concentrations whereas reductive quenching was dominant at higher concentrations. Therefore, it can be concluded that the photochemical dehydrogenation of formic acid using the proposed system occurs readily when oxidative quenching is dominant. It should be noted that the formation of HBIH cation via the reaction between BIH and formic acid can also deaccelerate the catalysis as the concentration of protons to react with the postulated hydride intermediate (*vide infra*) decreases to some extent.

Based on the results described above as well as those of previous reports on the dehydrogenation of formic acid, a possible mechanism for the described catalytic system based on **Co5** is proposed (see Scheme 1). First, a single cobalt ion in the triangular core of **Co5**, which exhibits a pentacoordinated structure, is reduced by $Ir(ppy)_3$ through oxidative quenching. Based on the experimental results, including the dependence of the catalytic performance of **Co5** on the choice of the photosensitiser (Fig. 3(b)) and the CV measurements of **Co5** performed in the presence of formic acid (Fig. S4), it can be concluded that the one-electron reduced species of **Co5** is the key active species in the reaction. This one-electron reduced species reacts with formic acid and releases hydrogen and CO_2 (HCOOH dehydrogenation). That CO_2 is formed during the catalysis process was confirmed using gas chromatography (Fig. S8). In this process, it is assumed that Co^I promotes the elimination of the C-H bond, like other cobalt complexes that catalyse formic acid dehydrogenation reactions.[2d,n] Moreover, it has been reported that the synergistic effects between the distinct metal ions play an important role in the dehydrogenation reaction[2n-p,7]. Thus, the multinuclear metal structure of **Co5** is an effective one for catalysis.

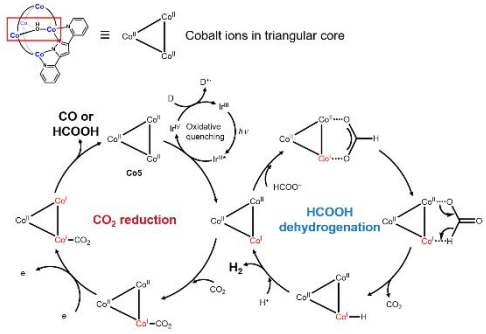

Scheme 1 Proposed mechanism of dual catalysis process mediated by **Co5**. Dehydrogenation of formic acid (right) and two-electron reduction of CO_2 (left).

In addition to participating in the formic acid dehydrogenation reaction, the one-electron reduced species of **Co5** also reacts with the CO_2 generated during the dehydrogenation reaction. The species receives a single electron from the photosensitiser and reduces CO_2 to formic acid or carbon monoxide (CO_2 reduction process)[6]. This CO_2 reduction process requires the injection of one more electron into the catalyst. To be able to access this two-electron-reduced species, electron transfer from the photosensitiser to **Co5** is necessary. Therefore, it can be assumed that the CO_2 reduction reaction will be accelerated under conditions where photoinduced electron transfer events occur frequently. As mentioned above, the concentration of $Ir(ppy)_3$ can be used to control the frequency of the photoinduced electron transfer events. Indeed, the amount of CO_2 detected depended primarily on the concentration of $Ir(ppy)_3$. On increasing the concentration of $Ir(ppy)_3$, the amount of CO_2 detected decreased (Fig. S8), even though the amount of hydrogen generated by the dehydrogenation of formic acid increased. This might indicate that the CO_2 formed by the dehydrogenation of formic acid was consumed by the CO_2 reduction process[8]. Thus, the dual catalysis mechanism explains both the dehydrogenation of formic acid and the two-electron reduction of CO_2 mediated by **Co5**.

Finally, we optimised the reaction conditions for the formic acid dehydrogenation reaction. By decreasing the concentration of BIH to 25 mM and increasing that of formic acid to 25 mM and performing photoirradiation with an Xe lamp ($420 < \lambda < 750$ nm), the maximum turnover number for the reaction could be increased to 229 after 1 h (Fig. S9). The turnover frequency (TOF, 229 h^{-1}) under this condition is the highest observed for molecular catalysts that operate under photoirradiation at ambient temperature (Table S4 and Fig. S10).

In conclusion, we have revealed the catalytic activity of a pentanuclear cobalt complex (**Co5**) for the photoinduced dehydrogenation of formic acid. The dehydrogenation reactions were performed under photoirradiation in the presence of **Co5** and a suitable photosensitiser at ambient temperature and resulted in the generation of hydrogen and CO_2. This is a rare example of the photoinduced dehydrogenation of formic acid under ambient conditions. In addition, it was determined that the activity of **Co5** is higher than those of similar previously reported molecular catalysts. Mechanistic investigations indicated that the one-electron-reduced species of **Co5** plays an essential role in the catalytic cycle. Given that **Co5** also catalyses the photochemical two-electron reduction of CO_2 into formic acid, this study is the first example of a hydrogen storage/release cycle based on the photochemical reduction of CO_2 and dehydrogenation of formic acid.

This work was supported by Grants-in-Aid for Scientific Research (KAKENHI) (Grant Numbers 17H06444, 19H00903, and 20K21209 (S.M.)), (Grant Numbers 15H05480, 17K19185, 17H05391, 19H04602, 19H05777, and 20H02754 (M. K.)), and (Grant Number 20K15955 (Y.S.)) from the Japan Society for the Promotion of Science. This work was also supported by JST PRESTO (Grant Number JPMJPR20A4 (M. K.)), JST CREST (Grant Number JPMJCR20B6 (S. M.)) and JST SPRING (Grant Number JPMJSP2138 (T. A.)), Japan, Iketani Science and Technology Foundation, the Izumi Science and Technology Foundation, and the Mazda Foundation (M. K.).

Conflicts of interest

There are no conflicts to declare.

Notes and references

1 K. Sordakis, C. Tang, L. K. Vogt, H. Junge, P. J. Dyson, M. Beller and G. Laurenczy, *Chem. Rev.*, 2018, **118**, 372.

2 (a) M. Iglesias and L. A. Oro, *Eur. J. Inorg. Chem.*, 2018, **2018**, 2125. (b) C. Guan, Y. Pan, T. Zhang, M. J. Ajitha and K. -W. Huang, *Chem. Asian J.*, 2020, **15**, 937. (c) R. S. Coffey, *Chem. Commun. (London)*, 1967, 923b. (d) M. Onishi, *J. Mol. Catal.*, 1993, **80**, 145. (e) C. Fellay, P. J. Dyson and G. Laurenczy, *Angew. Chem. Int. Ed.*, 2008, **47**, 3966. (f) B. Loges, A. Boddien, H. Junge, J. R. Noyes, W. Baumann and M. Beller, *Chem. Commun.*, 2009, 4185. (g) S. Fukuzumi, T. Kobayashi and T. Suenobu, *J. Am. Chem. Soc.*, 2010, **132**, 1496. (h) A. Boddien, F. Gärtner, R. Jackstell, H. Junge, A. Spannenberg, W. Baumann, R. Ludwig and M. Beller, *Angew. Chem. Int. Ed.*, 2010, **49**, 8993. (i) A. Boddien, B. Loges, F. Gärtner, C. Torborg, K. Fumino, H. Junge, R. Ludwig and M. Beller, *J. Am. Chem. Soc.*, 2010, **132**, 8924. (j) A. Boddien, D. Mellmann, F. Gärtner, R. Jackstell, H. Junge, P.J. Dyson, G. Laurenczy, R. Ludwig and M. Beller, *Science*, 2011, **333**, 1733. (k) C. -H. Chang, M. -H. Chen, W. -S. Du, J. Gliniak, J. -H. Lin, H. -H. Wu, H. -F. Chan, J. -S. K. Yu and T. -K. Wu, *Chem. Eur. J.*, 2015, **21**, 6617. (l) S. M. Barrett, S. A. Slattery and A. J. M. Miller, *ACS Catal.*, 2015, **5**, 6320. (m) M. A. Esteruelas, C. García-Yebra, J. Martín and E. Oñate, *ACS Catal.*, 2018, **8**, 11314. (n) W. Zhou, Z. Wei, A. Spannenberg, H. Jiao, K. Junge, H. Junge and M. Beller, *Chem. Eur. J.*, 2019, **25**, 8459. (o) Y. Sofue, K. Nomura and A. Inagaki, *Chem. Commun.*, 2020, **56**, 4519. (p) D. Hong, Y. Shimoyama, Y. Ohgomori, R. Kanega, H. Kotani, T. Ishizuka, Y. Kon, Y. Himeda and T. Kojima, *Inorg. Chem.*, 2020, **59**, 11976.

3 (a) A. Boddien, F. Gärtner, C. Federsel, P. Sponholz, D. Mellmann, R. Jackstell, H. Junge and M. Beller, *Angew. Chem. Int. Ed.*, 2011, **50**, 6411. (b) E. A. Bielinski, P. O. Lagaditis, Y. Zhang, B. Q. Mercado, C. Würtele, W. H. Bernskoetter, N. Hazari and S. Schneider, *J. Am. Chem. Soc.*, 2014, **136**, 10234. (c) Y. Zhang, A. D. MacIntosh, J. L. Wong, E. A. Bielinski, P. G. Williard, B. Q. Mercado, N. Hazari and W. H. Bernskoetter, *Chem. Sci.*, 2015, **6**, 4291. (d) S. Enthaler, A. Brück, A. Kammer, H. Junge, E. Irran and S. Gülak, *ChemCatChem*, 2015, **7**, 65. (e) J. B. Geri, J. L. Ciatti and N. K. Szymczak, *Chem. Commun.*, 2018, **54**, 7790.

4 (a) R. Tanaka, M. Yamashita and K. Nozaki, *J. Am. Chem. Soc.*, 2009, **131**, 14168. (b) C. A. Huff and M. S. Sanford, *ACS Catal.*, 2013, **3**, 2412.

5 (a) Y. Yamazaki, H. Takeda and O. Ishitani, *J. Photochem. Photobiol. C.*, 2015, **25**, 106. (b) H. Takeda, C. Cometto, O. Ishitani and M. Robert, *ACS Catal.*, 2017, **7**, 70. (c) H. Takeda, H. Koizumi, K. Okamoto and O. Ishitani, *Chem. Commun.*, 2014, **50**, 1491. (d) S. E. Lee, A. Nasirian, Y. E. Kim, P. T. Fard, Y. Kim, B. Jeong, S. -J. Kim, J. -O. Baeg and J. Kim, *J. Am. Chem. Soc.*, 2020, **142**, 19142.

6 T. Akai, M. Kondo, S. K. Lee, H. Izu, T. Enomoto, M. Okamura, Y. Saga and S. Masaoka, *Dalton Trans.*, 2020, **49**, 1384.

7 A. Zavras, M. Krstić, P. Dugourd, V. Bonačić-Koutecký and R. A. J. O'Hair, *ChemCatChem*, 2017, **9**, 1298.

8 There is no quantitative information on how much CO_2 accumulates in the solution before the reaction starts.